

On the Geometric Accuracy in Shallow Sloped Parts in Single Point Incremental Forming

Amirahmad Mohammadi^{1,a}, Hans Vanhove^{1,b}, Albert Van Bael^{2,c}
and Joost R. Duflou^{1,d}

¹KULeuven, Department of Mechanical Engineering, Belgium

²KU Leuven, Department of Metallurgy and Materials Engineering, Belgium

^aamirahmad.mohammadi@mech.kuleuven.be, ^bhans.vanhove@mech.kuleuven.be,

^calbert.vanbael@mtm.kuleuven.be, ^djoost.duflou@mech.kuleuven.be

Keywords: SPIF, accuracy, bulging, finite element modeling

Abstract. Incremental sheet forming is a versatile manufacturing technology for small series production. This technique is, however, still challenged by limited accuracy. In incremental forming, each shape comes with its unique complexity and typical geometrical deviations. In this work, the applicability of FE modeling for the prediction of geometric inaccuracies in a shallow wall angle cone has been studied. Typical geometric inaccuracies for shallow sloped parts have been investigated both experimentally and by means of simulation. The evolution of underforming of the cone base as well as overforming of the cone wall during SPIF forming of a truncated cone have been analyzed. Based on the evaluation of the contact zone between the tool and the sheet, it has been concluded that an extended deformation of the sheet outside the tool contact zone is responsible for the overforming of the wall.

Introduction

Single Point Incremental Forming (SPIF) is a dieless production technique in which sheets are progressively formed until a target 3D shape is achieved. Although SPIF is a versatile forming process, suitable for unique and small-batch production, extreme thinning and low accuracy obstruct its application on an industrial scale. In order to overcome these shortcomings, several approaches, from advanced work piece analysis techniques to the introduction of intelligent tool path strategies, have been proposed and applied [1,2,3].

FE-modeling enables an in-depth analysis of the forming mechanisms in SPIF and allows better understanding of the cause of formability limits and geometrical inaccuracy. Due to the local nature of the constantly moving deformation zone and the lengthy toolpaths, the modeling of large parts is extremely computationally demanding and not feasible within a reasonable time frame. For this reason and considering that a partial FE-model affects the prediction accuracy, SPIF simulations have mostly been carried out on small benchmark geometries. Additionally the use of shell elements, explicit finite element methods with mass/time scaling and adaptive remeshing contribute to further decrease of the CPU time.

Geometric inaccuracy is greatly dependent on material and geometry. Hussain et al. [4] used design of experiments to identify influencing factors on the amount of underforming of the bottom of SPIF formed parts. He concluded that increasing sheet thickness as well as material hardening (by material selection) increases the height of the underforming of the bottom, while increasing the wall angle reduces its size. Ambrogio et al. [5] proposed a smaller tool size and stepdown for improving the geometric accuracy of a 60° cone made in AA1050-O.

For reducing the underforming of the bottom, Essa et al. [6] proposed processing the entire cone base after the cone wall is formed. In this way, by a circular movement of the forming tool and a second moving supporting tool on the other side of the sheet, a flat bottom can be achieved at the

cone base. In addition, it has been concluded that by using a dynamic supporting tool, local springback reduces and a better geometric accuracy is achieved.

Analysis of the forming forces and the tool-sheet contact zone during the SPIF process contributes to understanding bulge formation in the base of a cone. Aerens et al. [7] showed that for low wall angled cones, the overall radial force on the tool is directed away from the centre of the part during incremental forming. Eyckens et al. [8] studied the contact area between the tool and the sheet for shallow and high wall angle cones using a submodeling technique. Simulation results show that for high wall angle cones, a line contact, which is elongated from the cone base towards the cone wall, can be observed, while for shallow wall angle cones the contact zone is more compact and positioned in the cone bottom region.

Although several efforts have been reported on the improvement of geometric accuracy in the SPIF process, no thorough in-depth analysis of inaccuracy formation for shallow sloped SPIF parts could be traced in literature. In this work, the evolution of geometric errors during the forming of a shallow wall angled cone has been studied using FE-modeling.

Experimental procedure

The material selected for this study is 1.25mm thick AA 5182-O alloy. This material is a solid-solution strengthening alloy which is extensively used for automotive structural components.

For studying the typical deviations that appear in shallow sloped parts, a 20° cone has been formed from a square sheet of 220 mm by 220 mm which was clamped at its perimeter. Fig. 1 shows the dimensions of the cone which was made in a backing plate containing a circular orifice with a diameter of 130 mm. The experiment has been conducted using a tool diameter of 10 mm, forming speed of 2000 mm/min and 16 stepdowns of 0.75 mm in Y-direction. The tool movement after each contour has been selected to be 'direct on part' (i.e. the shortest path between consecutive contours). The single point incrementally formed cone was measured by means of a line scanner with an accuracy of 20 µm and then compared with the original CAD model and simulated geometry.

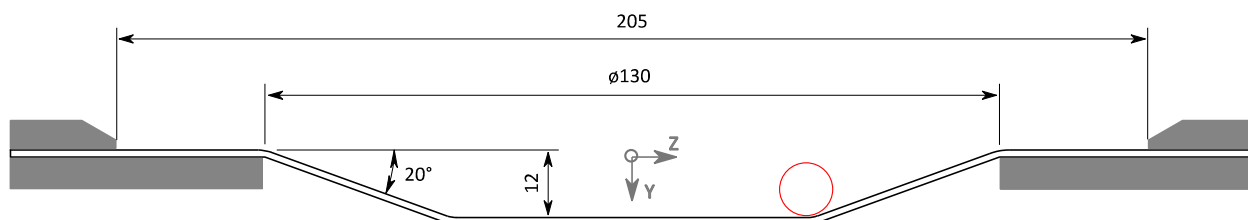


Fig. 1: Section view of a truncated cone and its nominal dimensions.

Finite element model description

An explicit solver of ABAQUS has been used to simulate the incremental forming of a 20° cone. This method is preferred over an implicit method since taking larger increment steps is computationally more expensive. The forming tool and the backing plate were modeled as 3D analytical rigid surfaces and the sheet metal has been meshed using a 4-node shell element (S4R) with five integration points over the thickness (element size = 2 mm). This type of element can be successfully used because of a negligible through thickness shear in shallow wall angle geometries [9].

The blank holder has been modeled by constraining the corresponding translational and rotational degrees of freedom (DOF) of the nodes along the edges, while the forming tool movement has been simulated based on the actual SPIF toolpath.

The sheet material is considered as elastic–plastic material and the isotropic Swift hardening law and Von Mises yield criterion have been applied for the FE-model (see Table 1). Coulomb friction models with friction coefficients of 0.05 between tool and blank (lubricated contact), and 0.15 between blank and backing plate (dry contact) have been applied.

Table 1 Material parameters for AA 5182-O [10].

Density [Kg/m ³]	Young's modulus [MPa]	Poisson ratio [-]	$\sigma = K \varepsilon^n$	
			K [MPa]	n [-]
2700	7e+4	0.3	540	0.304

With:

K: strength coefficient

n: hardening exponent

ε : equivalent plastic strain

Results and discussion

Validation of the predicted geometry and thickness. Fig. 2 presents a section view (YZ-plane) of the simulated and experimental geometries. Comparison of results shows that the geometry of the cone can be well predicted by the used FE model. It can be observed that the bulging of the bottom (see A in Fig. 3(a)) is underestimated by about 8% in the FE simulation, while the overforming of the cone wall is slightly underestimated. However, the underforming of the cone base (see B in Fig. 3(a)) and sheet metal bending close to the backing plate (see D in Fig. 3(a)) are well predicted by the simulation. The small differences between the experimental and simulation results can be explained by the selection of a simple isotropic hardening model without considering cyclic hardening.

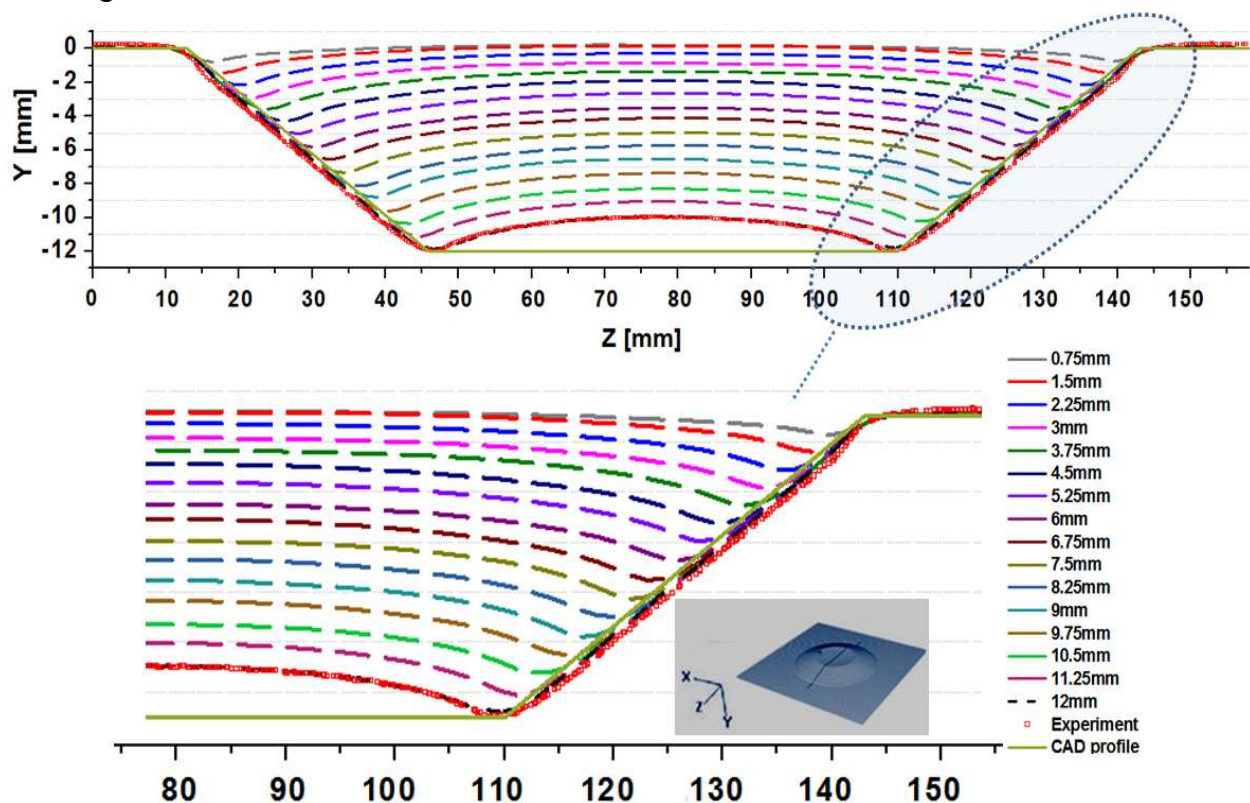


Fig. 2. A comparison between predicted geometry, experimentally formed part and CAD profile along the YZ-plane. The dashed lines represent the predicted geometry after each contour.

Note: The cone has been formed using 16 toolpath contours.

The deformation of the blank is in a stepwise fashion with an incremental increase per contour. The total deformation of the blank after forming together with the underforming of the cone base can be seen in Fig. 4(a). Fig. 4 (b) shows the equivalent plastic strain in the cone after forming. It is observed that, due to the shallow wall angle of the deformed geometry, the maximum value in the blank is limited to 0.43. The maximum plastic strains are observed in the stepdown and in the regions close to the square clamping plates (i.e. at 90°, 180° and 270° to the stepdown position). Results of the thickness distribution, shown in Fig. 4(c-d), also confirm that the maximum thinning is reached in the stepdown region. The predicted thickness distribution results are in good agreement with experimental data and a minimum thickness of 1.1 mm is obtained in both cases.

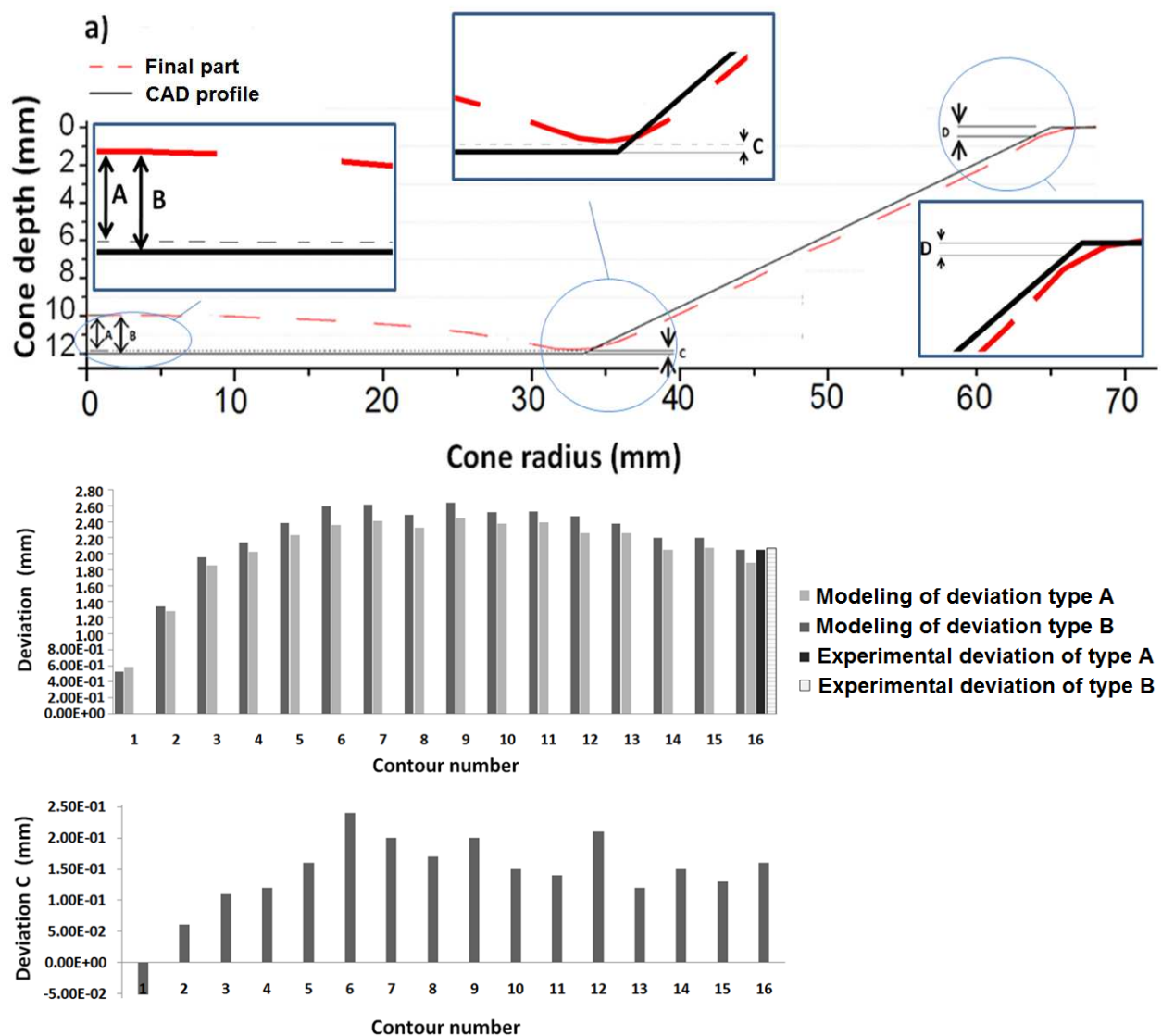


Fig. 3. a) Schematic of different types of inaccuracy in the deformed geometry, b) Simulated and experimental values of A and B, c) Simulated value of C.

- A: Bulging of the bottom
- B: Underforming of the bottom
- C: Underforming of the corner
- D: Bending close to the backing plate

Bulge formation. Fig. 2 shows the deformation of the blank after the full forming procedure and the simulated evolution of the forming process. To evaluate the results, different types of geometrical inaccuracies have been identified and measured at each contour (see Fig. 3. (a)). It has been observed that the bulging (see A in Fig. 3.(a)), the underforming of the cone base (see B in Fig. 3.(a)) and the deformation of the cone corner (see C in Fig. 3.(a)) are already initiated from the first contours and continue to increase till contour No.6 (cone depth of 4.5 mm). From contour No.6 onward, the underforming and bulge height show a decreasing trend. Further study is needed to understand the reasons for this observed evolution of the bulging behavior.

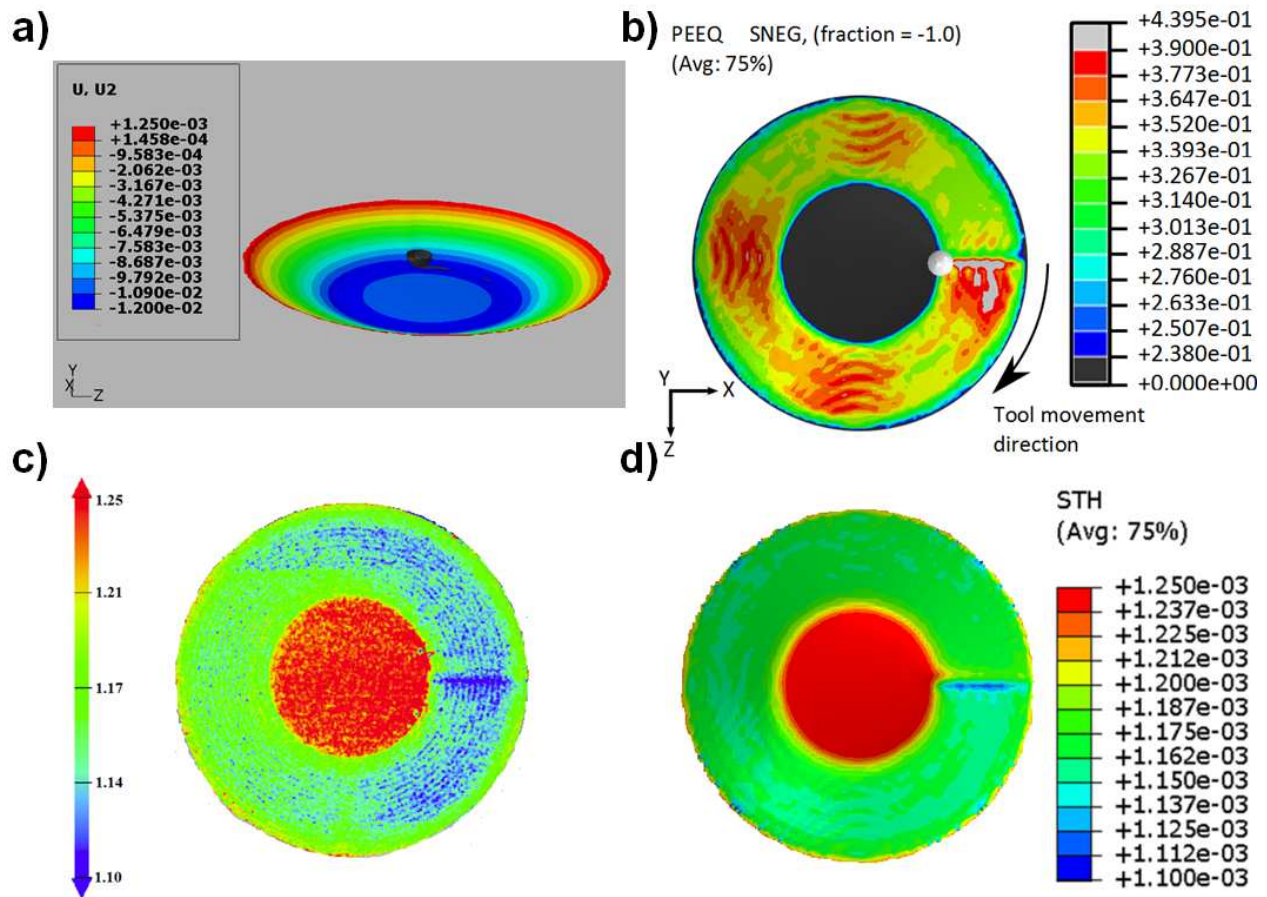


Fig. 4. a) Displacement along Y-axis, b) Equivalent plastic strain distributions, c) Experimental thickness and d) Predicted thickness.

Overforming of the cone wall. For studying the earlier observed overforming of the wall, the deformation history of a selected node on the cone wall region (see Fig. 5) has been recorded during the SPIF process using FE simulation.

Fig. 6 shows a node displacement along the Y-axis (direction of tool axis) during all 32 timesteps of the forming process. These 32 steps consist of 16 contour steps and 16 stepdown steps. Simulation results show that the forming tool contacts the chosen node after 17.75s which corresponds to a cone depth of 6.75 mm. Immediately after the tool moves away from the node within the same contour, the node moves upward due to the local elastic springback and a rigid body motion of the sheet. By further forming of the sheet in subsequent contours (i.e. step 20 and onward), the node continues to move in Y- direction. This extended displacement increases over a series of subsequent steps till timestep 24. It is interesting to note that no significant extended displacement of the node was measured in radial or tangential direction.

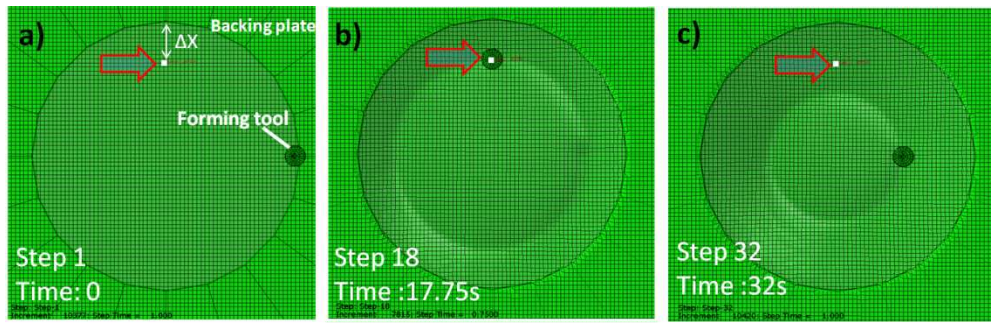


Fig. 5. Node on the wall of the cone at different steps of the forming process (an arrow pointing to the node at 19.9×10^{-3} m from backing plate)

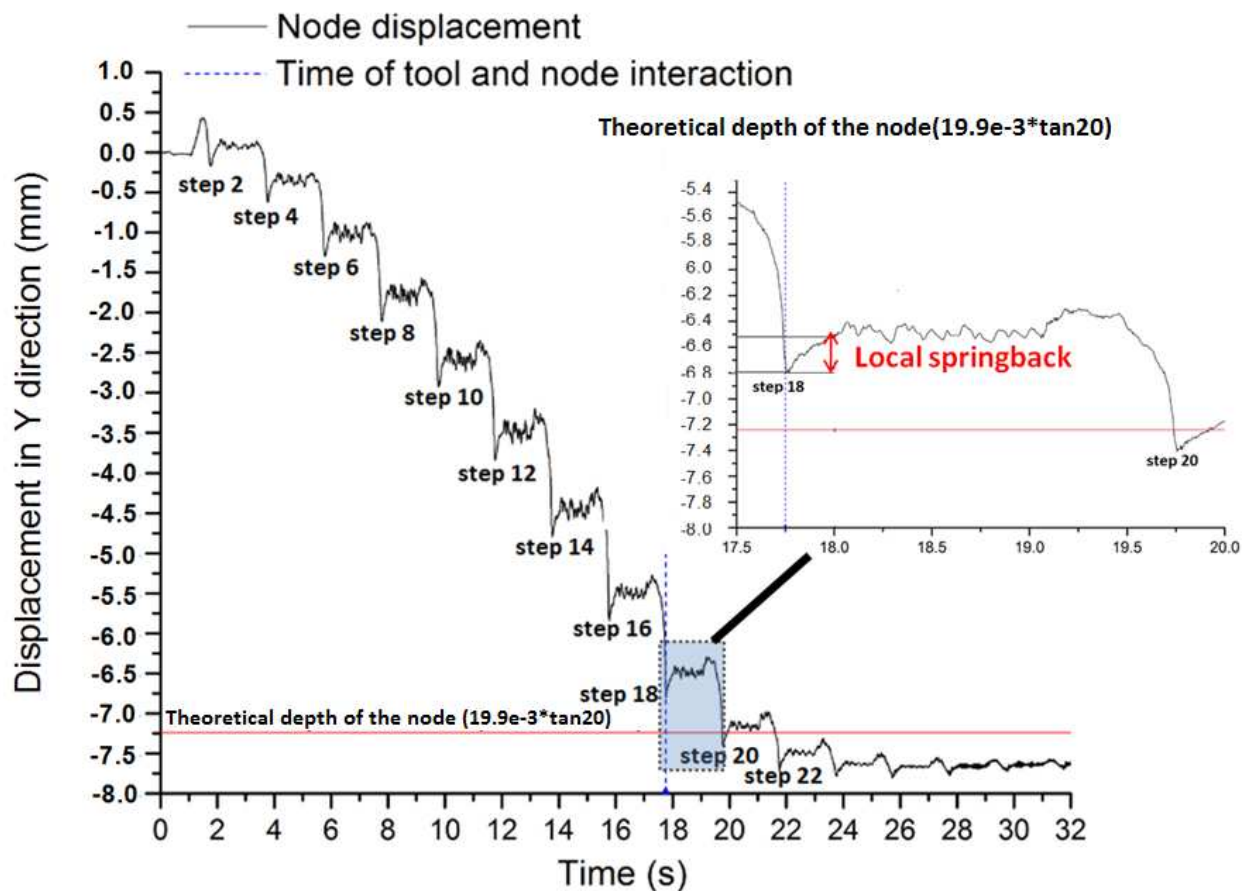


Fig. 6. Node displacement during forming.

From studying the distribution of the contact pressure between the sheet metal and the tool, it has been observed that after the tool passed the node, no contact is developed between the tool and the node in subsequent forming steps. This is because the tool is mostly in contact with the sheet in the cone base rather than the cone wall region and there is always a forward and slightly inward offset between the compact contact zone and the center of the forming tool (see Fig. 7). Therefore, the plastic deformation formed after timestep 18, which results in overforming of the wall cannot be generated due to the repassing of the tool over the node region. This unwanted plastic deformation, resulting in a downwards displacement of the node and observed as overforming in the final workpiece, is caused by the fact that the tool contact zone is positioned slightly on the inside of the tool and thus on the bulged bottom of the sheet.

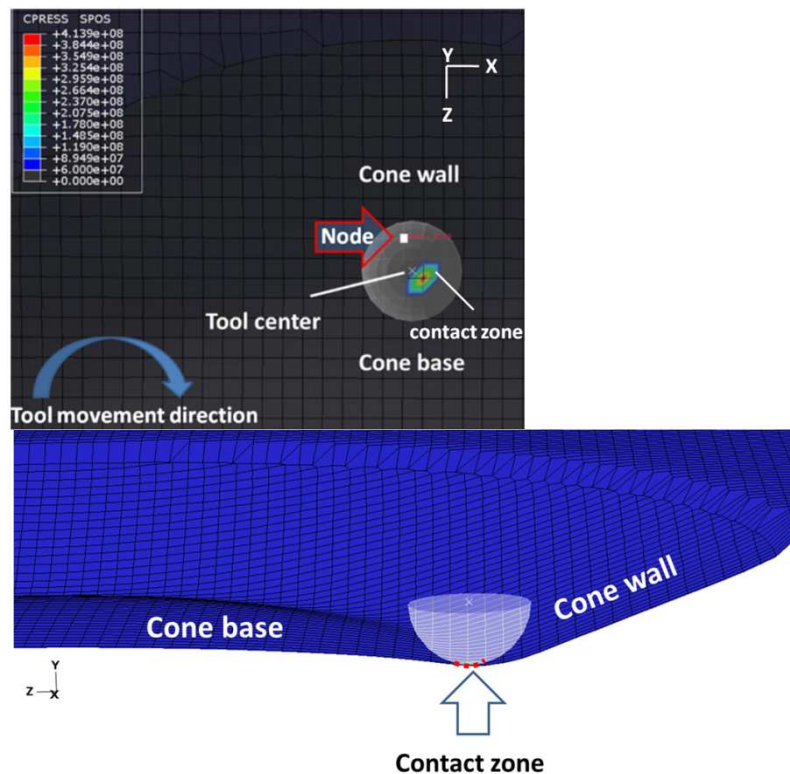


Fig. 7. The distribution of the contact pressure beneath the forming tool at step 22 (cone depth of 8.25 mm).

Conclusion

In order to better understand the material behavior during the production of shallow sloped parts, FEA simulations have been used. In this study FEA has shown to provide accurate predictions of final accuracy and thickness distribution. The simulation of the bulge evolution during forming shows an initial increasing bulging of the bottom of a shallow sloped cone until it reaches its maximum around a cone depth of 4.5 mm, after which it slowly decreases again. Through simulated material flow and tool contact area, it can be seen that the sheet keeps significantly moving in a general downward direction in the succeeding contours after tool contact. This can be explained by the tool contact zone being on the bulged bottom which causes an overforming of the walls of shallow sloped parts.

References

- [1] G., Hirt, J., Ames, M., Bambach and R., Kopp, Forming strategies and Process modelling for CNC Incremental sheet forming, *Annals of the CIRP*, 53, 1, (2004) 203-206.
- [2] F. Micari, G. Ambrogio and L. Filice, Shape and dimensional accuracy in single point incremental forming: state of the art and future trends, *J. Mater. Process. Technol.*, 191 (2007) 390-395.
- [3] J. Verbert, A. Behera, B.Lauwers, J. Duflou, Multivariate Adaptive Regression Splines as a Tool to Improve the Accuracy of Parts Produced by FSPIF. 473, (2011) 841-846.
- [4] G. Hussain, L. Gao, N. Hayat, Improving profile accuracy in SPIF through statistical optimization of forming parameters, *Journal of Mechanical Science and Technology*, 25 (2010), 77-82.
- [5] G. Ambrogio, I. Costantino, L. De Napoli, L. Filice, M. Muzzupappa, Influence of some relevant process parameters on the dimensional accuracy in incremental forming: a numerical and experimental investigation, *Int. J. Mater. Process. Technol.*, 153-154/C (2004) 501-507.

- [6] K. Essa, P. Hartley, An assessment of various process strategies for improving precision in single point incremental forming, *International Journal of Material Forming*, (2010) DOI 10.1007/s12289-010-1004-9.
- [7] R. Aerens, P. Eyckens, A. Van Bael, J. R. Duflou, Force prediction for single point incremental forming deduced from experimental and FEM observations, *International Journal of Advanced Manufacturing Technology*, 46 (2010) 969-982.
- [8] P. Eyckens, A. Van Bael, R. Aerens, J. R. Duflou, P. Van Houtte, Small-scale Finite Element Modelling of the Plastic Deformation Zone in the Incremental Forming, *International Journal of Material Forming*, 1 (2008) 1159-1162.
- [9] P. Eyckens, J. Moreau, J. R. Duflou, A. Van Bael, P. Van Houtte, MK modelling of sheet formability in the incremental sheet forming process, taking into account through-thickness shear, *International Journal of Material Forming*, 2 (2009) 370-382.
- [10] N. Abedrabbo, F. Pourboghrat, J. Carsley, Forming of AA5182-O and AA5754-O at Elevated Temperatures using Coupled Thermo-Mechanical Finite Element Models, *Int. J. Plasticity*, 23 (2007) 841-875.

The Current State-of-the-Art on Material Forming

10.4028/www.scientific.net/KEM.554-557

On the Geometric Accuracy in Shallow Sloped Parts in Single Point Incremental Forming

10.4028/www.scientific.net/KEM.554-557.1443